Coexisting spin-flop coupling and exchange bias in LaFeO_{3}/La_{0.7}Sr_{0.3}MnO_{3} heterostructures

F. K. Olsen, I. Hallsteinsen, E. Arenholz, T. Tybell, and E. Folven

Coexisting spin-flop coupling and exchange bias in $LaFeO_3/La_{0.7}Sr_{0.3}MnO_3$ heterostructures

F.K. Olsen,[1] I. Hallsteinsen,[1,2] E. Arenholz,[2] T. Tybell,[1] and E. Folven[1]

[1]*Department of Electronic Systems, NTNU – Norwegian University of Science and Technology, 7491 Trondheim, Norway*

[2]*Advanced Light Source, Lawrence Berkeley National Laboratory, Berkeley, California 95616, USA*

Exchange bias occurs in field-cooled antiferromagnet/ferromagnet systems and can most often be explained in terms of uncompensated magnetic moments at the interface, that are pinned in their orientation during field-cooling. The presence of spin-flop coupling is often associated with spin-compensated interfaces. Here, we report exchange bias in complex oxide heterostructures of antiferromagnetic $LaFeO_3$ and thin layers of ferromagnetic $La_{0.7}Sr_{0.3}MnO_3$ with several intriguing features. The exchange bias does not require field cooling but can also be obtained by applying a setting field at elevated temperature. Furthermore, the exchange bias is positive for setting fields up to 3 T, and its magnitude is strongly dependent on the setting field strength. X-ray magnetic linear dichroism measurements show a predominantly perpendicular spin configuration at the interface. We discuss the possibility of the exchange bias being driven by a net moment from spin canting in the antiferromagnet due to Dzyaloshinkii-Moriya interactions.

I. INTRODUCTION

Complex oxide heterostructures and their interfaces offer a wide range of new and unexpected phenomena with potential for utilization in modern devices.[1] In highly correlated electron systems, interfacial magnetic frustration, discontinuity of electron states and strain- or charge transfer induced orbital reconstructions may give rise to new ground states and functional properties.[2,3] Phenomena such as superconductivity, colossal magnetoresistance, metal-insulator transitions and multiferroicity have attracted much attention over the last decades,[4-6] and recent developments in modern material synthesis have enabled research on tuning of these functional properties using interface engineering.

At the interface between a ferromagnet (FM) and an antiferromagnet (AF), exchange coupling of the FM and AF spin lattices can give rise to increased coercivity in the FM layer and in some cases induce a unidirectional anisotropy or exchange bias (EB).[7] Due to its technological relevance, the EB effect has attracted much attention since its discovery but its origin in diverse systems is still researched extensively today.[8-10] In most systems EB is obtained by field cooling (FC) the AF/FM system through the AF ordering temperature, T_N. However, spontaneous EB that does not require field cooling has been reported, e.g., in $Fe/Cr_2O_3/Fe$ trilayers[11] and Ni-Mn-Sn alloys[12] and recently also in perovskite systems such as polycrystalline $La_{1.5}Sr_{0.5}CoMnO_6$,[13] and $La_{0.7}Sr_{0.3}MnO_3/Eu_{0.45}Sr_{0.55}MnO_3$ heterostructures.[14] A shift of the hysteresis loop in the opposite direction of the cooling field is most commonly observed (negative EB), but a loop shift in the cooling field direction (positive EB) has also been reported.[15-18]

Theoretical models often explain EB by the presence of uncompensated magnetic moments at the interface. These uncompensated moments could result either from the bulk-truncated spin structure or, in cases where a spin-compensated AF surface is expected, from defects, surface roughness, AF spin canting, or induced FM- or spin glass order in the antiferromagnet.[8-10,19] Furthermore, Dong et al. predicted that Dzyaloshinkii-Moriya interactions (DMI) could give rise to EB in G-type AF/FM perovskite heterostructures with spin compensated interfaces,[20] and EB was later observed experimentally in the $SrMnO_3/La_{2/3}Sr_{1/3}MnO_3$ system.[21] Since DMI in perovskites are closely linked to the extent of octahedral rotations, epitaxial strain can be used to modify the interaction, which enables engineering of EB in perovskites.

In many systems showing EB, the spin coupling across the AF/FM interface is reported to be collinear and EB is explained in terms of an imbalance in the number of parallel and antiparallel aligned spins. For some spin-compensated AF/FM systems, a spin-flop coupling is found, i.e. the AF spin axis is aligned perpendicular to the FM spin axis.[22] The spin-flop coupling is highly sensitive to imperfections in the spin-compensation, which would cause a transition to collinear coupling,[10] and most EB systems are reported to show collinear coupling. However, coexisting EB and spin-flop alignment has also been found, e.g., in the ferrimagnetic/AF system of Fe_3O_4/CoO where DMI is proposed to give rise to uncompensated moments.[23]

Here, we report positive EB which can be set without FC through a magnetic ordering temperature in $LaFeO_3/La_{0.7}Sr_{0.3}MnO_3$ (LFO/LSMO) heterostructures grown epitaxially on (001)-oriented $SrTiO_3$ (STO). The G-type AF order in LFO gives rise to a fully spin compensated interfacial plane, and spin-flop coupling has been demonstrated in several experimental studies.[24,25] LFO is known to exhibit DMI which causes weak ferromagnetism,[26] but EB has not been reported in this epitaxial system before. We discuss how spin canting in LFO can give rise to a net moment at the interface, explaining the EB, without breaking the spin-flop state in this system.

II. EXPERIMENTAL

Epitaxial LSMO films and LFO/LSMO heterostructures were grown on (001)-oriented STO using pulsed laser deposition. Samples investigated by x-ray spectroscopy were grown on conducting STO substrates doped with 0.05 wt% Nb to avoid charging. A KrF excimer laser (λ=248 nm) with a fluency of $\sim$ 2 J/m^2 and frequency of 1 Hz (LSMO) and 5 Hz (LFO) was used. Oxide layers were deposited at 700 °C (LSMO) and 540 °C (LFO) in oxygen pressures of 0.35 mbar (LSMO) and 0.01 mbar (LFO). In-situ reflection high energy electron diffraction (RHEED) showed monolayer oscillations throughout the growth. After deposition, the samples were annealed in an oxygen pressure of 100 mbar for 15 minutes. LSMO samples were grown with layer thicknesses of 10 u.c. (unit cells), 15 u.c., 20 u.c., 40 u.c. and 112 u.c. (4 nm - 43 nm), and heterostructures with fixed LFO thickness of 10 u.c. (4 nm) and LSMO thicknesses 8 u.c., 10 u.c., 15 u.c., 20 u.c. and 90 u.c. (3 nm – 35 nm) were synthesized. Atomic force microscopy (AFM) revealed surfaces with sub-monolayer roughness and step-edges inherited from the STO substrate. X-ray diffraction (XRD) measurements were performed on samples with thickness > 20 u.c. and showed LSMO layers fully strained to the STO substrate. Magnetization data was acquired using a Quantum Design vibrating sample magnetometer (VSM) in the temperature range 50-400 K. Care was taken to ensure that all experiments were conducted using the same cooling rate (20 K/min) and any external setting fields were applied using the same field ramping rate (20 mT/s). X-ray magnetic circular and linear dichroism measurements (XMCD and XMLD, respectively) were performed at beamline 4.0.2 at the Advanced Light Source, Lawrence Berkeley National Laboratory.

III. RESULTS AND DISCUSSION

Figure 1(a) shows the saturation magnetization as a function of temperature for the LFO/LSMO heterostructures together with a 112 u.c. single layer LSMO reference sample. Both volume magnetization, and the Curie temperature, T_C, show a strong dependence on LSMO thickness. This agrees well with previous studies where reduction of M and T_C for thin epitaxial LSMO layers on STO is explained in terms of a magnetically dead layer near the film-substrate interface, and an associated transition from a 3D to a 2D magnetic ordering.[27,28] For LFO thin films grown on (001) STO, $T_N = 670$ K.[29]

FM hysteresis loops for as-grown single layer LSMO and LFO/LSMO heterostructures measured at 50 K are shown in Fig. 1(b). The hysteresis loops are all symmetric around the origin and the heterostructures show a coercive field, H_C, an order of magnitude larger than that of single layer LSMO films. Enhanced coercivity is a common observation when ferromagnets are coupled to antiferromagnets, and our values correspond to those previously reported for LFO/LSMO heterostructures.[30] In LFO/LSMO samples with an LSMO thickness down to 10 u.c., single hysteresis loops are observed. However, the heterostructure with 8 u.c. LSMO shows signs of a double loop, suggesting possible EB in the system.

Upon FC from 400 K to 50 K in a 3 T field applied along the crystallographic [100] axis, hysteresis loops obtained at 50 K reveal pronounced EB in all heterostructures, except for the sample with a thick (90 u.c.) LSMO layer. The hysteresis loop shift is in the same direction as the cooling field, i.e. a positive EB is observed. Hysteresis loops for the LFO (10 u.c.)/LSMO (8 u.c.) heterostructure are shown in Fig. 2(a), where the EB shift is 29 mT after FC, for both directions of the setting field.

The dependence of the EB on cooling field strength is investigated by performing FC from 400 K ($>T_C$) to 50 K and subsequently measure hysteresis loops at 50 K, H_{EB}^{50K}, for the LFO (10 u.c.)/LSMO (8 u.c.) heterostructure, see Fig. 2(b). We find H_{EB}^{50K} to be positive for all cooling fields and increase monotonically with field strength up to 3 T. The biased loops are asymmetric around the loop center for all field strengths, which suggests that a 3 T field is not sufficient to fully saturate the bias. For the zero field cooled measurements shown in Fig.1(a), the two subloops in the hysteresis indicate that there are biased domains even after growth, but a balanced distribution of domains biased in different directions. As can be seen in the inset in Fig. 2(b), the subloop shifted in the cooling field direction grows at the expense of the other upon FC. This indicates that all domains generate a positive EB and that the ones aligned with the cooling field grow with increasing field strength. Positive EB can be explained by a net magnetic moment at the interface which favors antiparallel coupling to the bulk FM moment. We note that Bruno et al. have recently reported induced FM moments on Fe at the LFO/LSMO interface.[30] These moments are only present below T_C and couple antiparallel to the Mn moments in LSMO. However, as these induced moments are found to follow the rotation of the LSMO moments, they do not give rise to EB.

The temperature dependence of the observed EB is examined by gradually heating the samples from 50 K, after FC in 3 T, and measuring hysteresis loops in intervals of 25 K. The EB values obtained as a function of temperature are shown in Fig. 3(a). As the temperature is increased, a monotonic reduction of the EB is found up to a blocking temperature T_B, i.e., the temperature where the EB goes to zero. The T_B values for the different samples, indicated in Fig. 3(a), show no clear trend with film thickness and are found to be in the range 150-200 K. We find T_B to be lower than T_C for all LSMO thicknesses. These data indicate that T_B and the T_C of LSMO are not directly related.

The coercive field observed after FC is larger than for single LSMO films and decreases with increasing temperature, as shown in Fig. 3(b). We note that there is no obvious change in H_C at T_B. Compared to the single layer LSMO reference sample, enhanced H_C is also found above T_B while EB disappears. Our results indicate that the mechanisms that give rise to EB and increased H_C, respectively, have different temperature dependence and are of different origin.

After heating above T_B, even as high as 400 K, we still find a significant EB when the samples are cooled back down to 50 K in zero field. This result implies that the moment responsible for EB is not lost at T_B nor at T_C. Hence, neither of these temperatures correspond to the ordering temperature of the moment causing EB. This result also suggests that T_B in our system is not associated with a spin glass freezing temperature, as has been reported for similar systems showing EB.[31,32] Performing multiple (30x) field loops at 50 K does not result in any training of the system (data not shown). However, we find that the symmetric double loop, with no net EB, as shown in Fig. 1(b) can be regained by performing a demagnetizing cycle (i.e. alternating fields) at 400 K, starting at 3 T with decrements of 10 mT.

To further explore how EB behaves in this system, we apply different setting fields, H_{set}, at different temperatures, T_{set}, cool the sample in zero field and measure H_{EB}^{50K}. We find that the EB can be set without FC, i.e., the system features spontaneous EB, and that the magnitude of the EB depends on both H_{set} and T_{set}. Figure 4 (lower panel) shows the resulting H_{EB}^{50K} for the LFO (10 u.c.)/LSMO (8 u.c.) sample. We find three different regimes. For low T_{set}, the EB is "frozen", i.e., applied fields up to 3 T are insufficient to set any EB. For intermediate T_{set}, the EB can be partially set, i.e., the magnitude of the EB depends on the value of H_{set}. For high T_{set}, the EB can be fully saturated and we obtain the largest EB values, however a reduction in H_{EB}^{50K} is also found as T_{set} is increased above ~ 250 K. Figure 4 (upper panel) shows the H_{EB}^{50K} values for $H_{set} = 3$ T in detail together with the values obtained by FC from the same temperatures. Comparing the FC and zero-FC data, we find that no EB can be set at low temperature and intermediate T_{set} leads to similar H_{EB}^{50K} values for both cases. We also find a bifurcation point at intermediate T_{set}. While FC from temperatures above 250 K yields the same H_{EB}^{50K} as for 250 K, zero-FC yields largest H_{EB}^{50K} for $T_{set} = 250$ K but it is reduced as $T_{set} > 250$ K. The decreased values of H_{EB}^{50K} for higher T_{set} can be attributed increased thermal fluctuations, i.e., the moment which causes EB is effectively reduced when the applied magnetic field is removed. Since the field is not removed in the FC case, a larger H_{EB}^{50K} is obtained. Furthermore, we see from Fig. 4 (lower panel) that lowering T_{set} requires an increase in H_{set} in order to obtain similar EB values. We attribute this feature to an increase in coercivity for the magnetic moments responsible for the EB, as temperature is lowered. We also note that an EB can be set at 400 K without FC, which indicates that the ordering temperature of the moment causing EB is above this temperature.

The EB as function of LSMO thicknesses is shown in Fig. 5. An EB is only observed for LSMO thicknesses of 20 u.c. (8 nm) and below, and increases abruptly as the LSMO layer thickness is reduced. We apply a simple model following the original ideas of Meiklejohn and Bean, which relates the EB to the thickness of the FM layer.

$$H_{EB} = \frac{\sigma_{int}}{M_{FM} t_{FM}}$$

Here, σ_{int} is the effective interfacial energy density arising from the magnetic moments causing EB, and M_{FM} and t_{FM} are the FM magnetization and thickness respectively.[7,33,34] For a G-type antiferromagnet such as LFO, the (001) interface is ideally spin compensated. However, our experimental EB values for the different LSMO thicknesses correspond to σ_{int} in the range 7-15 $\mu J/m^2$. The average value $\sigma_{int} = 10.6\ \mu J/m^2$ is used to calculate the solid line in Fig. 5. We note that the EB and corresponding σ_{int} values are in the same range as reported in studies on metal/LFO systems, e.g., Fe/LFO and Co/LFO,[35,36] however, orders of magnitude lower than the theoretical predicted values for fully uncompensated interfaces. This suggests that the LFO/LSMO interface consists of only a fraction of uncompensated spins. σ_{int} can be expressed as $\sigma_{int} = J \vec{S}_{FM} \vec{S}_{AF}/a^2$, which includes the interface exchange interaction, J, between the interfacial spins $\vec{S}_{FM}$ and $\vec{S}_{FM}$ in the FM and AF layers and a which is the in-plane unit cell parameter of the AF. One possibility is that a fraction of the interfacial Fe spins couples antiparallel rather than spin-flop to the Mn spins in LSMO. In this situation the AF spins would not cancel and ~ 5 % of interfacial Fe spins being antiparallel ordered to LSMO would explain the observed EB effect. Even though neither VSM, nor XMCD measurements at the Mn and Fe L-edges performed at 300 K show any detectable FM moment (data not shown), we cannot exclude the possibility of a net moment at the interface, as only a small moment would be sufficient for a significant bias. Another possibility is that interfacial Fe spins are canted in-plane, which would yield a net magnetic moment and could produce an EB in LSMO.

To investigate the spin configuration for LFO/LSMO exhibiting EB, we perform XMLD spectroscopy on heterostructures with LSMO thickness 8 u.c., 10 u.c. and 15 u.c. An EB is set by applying a 3 T field along the crystallographic [100] direction at 300 K, and the heterostructures are then cooled in zero field. The XMLD measurements are performed with x-rays incident perpendicular to the sample surface and an azimuthal orientation of the sample such that the linear polarization of the light coincides with a <100> axis, see Fig. 6(a). In this geometry, an XMLD signal will only arise if there is an imbalance in AF spins oriented along the in-plane [100] and [010] directions, respectively. The FM moment of LSMO is aligned to the in-plane [100] direction, by an external field. To avoid trapping of photoemitted electrons by the external field it is applied with an angle of 20° to the sample surface, see Fig. 6(a). The full Fe L-edge XAS spectra obtained from the heterostructure with 15 u.c. LSMO at 80 K using two linear polarizations are shown in Fig. 6(b) together with the XMLD difference. The sign of the XMLD signal at the L_2 edge corresponds to a majority of Fe spins aligned parallel to the [010]

direction.[25,37] As the FM is saturated along the [100] direction, there is a perpendicular alignment of Mn and Fe spins and we conclude we have coexisting spin-flop and EB in our system. The dichroism signals at the L_2 edge obtained at 80 K and 210 K for the three measured samples are shown in Fig. 6(c). For all three heterostructures we find a strong dichroism signal at 80 K and no evident dichroism signal at 210 K. The coexistence of EB and spin-flop at low temperatures together with the finding that the two phenomena vanishes in the same temperature range could suggest that spin-flop alignment and EB are related in this system.

The presence of EB and a predominantly perpendicular spin configuration at the LFO/LSMO interface could indicate DMI driven EB. This asymmetric exchange interaction adds another term to the total exchange energy:

$$H = \sum_{i,j}[J_{i,j}(\vec{S}_i \cdot \vec{S}_j) + \vec{D}_{ij} \cdot (\vec{S}_i \times \vec{S}_j)]$$

where $\vec{D}_{ij}$ is the DM vector related to two neighboring spins $\vec{S}_i$ and $\vec{S}_j$. Dong et al. have previously discussed how interfacial DMI, i.e., considering the term including $\vec{S}_{AF}$ and $\vec{S}_{FM}$ across the interface in a G-type AF/FM system can cause EB when the AF spin structure has a large out of plane component.[20] However, in the LFO/LSMO system, both the FM and AF spins are ideally in-plane, and hence the interface DMI term $\vec{D}_{AF,FM} \cdot (\vec{S}_{AF} \times \vec{S}_{FM})$ will not give rise to any net moment in our system. On the other hand, bulk LFO is known to exhibit spin canting and weak ferromagnetism due to DMI between neighboring AF spins.[26] We cannot exclude that at the LFO/LSMO interface, a net moment due to such spin canting may give rise to EB. In perovskites with reduced symmetry, like orthorhombic LFO, the octahedral rotations cause staggered B-O-B bonds which causes the direction of $\vec{D}_{ij}$ to alternate when moving along $\langle 100 \rangle_{pc}$. When the direction of $\vec{D}_{ij}$ coincides with a staggered AF spin structure a net moment will result. Considering the three principal axes of rotation, for a (001)-oriented interface plane it is the out-of-plane octahedral rotations, i.e., around the [001] axis which will cause a $\vec{D}_{ij}$ out-of-plane and lead to canting in-plane, see Fig. 7. If we assume that all interfacial Fe spins are canted by an equal amount, our experimental value of σ_{int} would correspond to a canting of ~ 3 deg, i.e. in deviation from perfect spin-flop. However, this would require a larger canting angle than that reported in bulk LFO of 0.521 deg.[26]

IV. SUMMARY

In summary, we report positive EB in epitaxial LFO/LSMO bilayers grown on (001) STO substrates. The EB persists up to a blocking temperature, T_B, which is similar for all LSMO layer thicknesses and lower than both T_C of LSMO and T_N of LFO. The EB does not require field cooling, and the direction and magnitude of the EB can be tuned by applying magnetic fields above T_B. The magnitude of the EB is dependent on the LSMO layer thickness. Element specific x-ray spectroscopy shows a predominant

perpendicular spin alignment at the AF/FM interface, which emerges together with the onset of EB at T_B. Finally, we discuss possible explanations for EB in a system with spin-flop coupling.

V. Acknowledgements

[1]   M. Lorenz *et al.*, J. Phys. D. **49** (2016).
[2]   H. Y. Hwang, Y. Iwasa, M. Kawasaki, B. Keimer, N. Nagaosa, and Y. Tokura, Nature Mater. **11**, 103 (2012).
[3]   A. Bhattacharya and S. J. May, Annu. Rev. Mater. Res. **44**, 65 (2014).
[4]   A. Ohtomo and H. Y. Hwang, Nature **427**, 423 (2004).
[5]   Y. Tokura, Rep. Prog. Phys. **69**, 797 (2006).
[6]   M. M. Vopson, Crit. Rev. Solid State Mater. Sci. **40**, 223 (2015).
[7]   W. H. Meiklejohn and C. P. Bean, Phys. Rev. **102**, 1413 (1956).
[8]   W. Zhang and K. M. Krishnan, Mater. Sci. Eng. R. **105**, 1 (2016).
[9]   M. Kiwi, J. Magn. Magn. Mater. **234**, 584 (2001).
[10]   A. E. Berkowitz and K. Takano, J. Magn. Magn. Mater. **200**, 552 (1999).
[11]   S. Sahoo, T. Mukherjee, K. D. Belashchenko, and C. Binek, Appl. Phys. Lett. **91** (2007).
[12]   B. M. Wang, Y. Liu, B. Xia, P. Ren, and L. Wang, J. Appl. Phys. **111** (2012).
[13]   J. K. Murthy and A. Venimadhav, Appl. Phys. Lett. **103** (2013).
[14]   J. K. Murthy and P. S. A. Kumar, Sci. Rep. **7**, 6919 (2017).
[15]   C. Shang, S. P. Guo, R. L. Wang, Z. G. Sun, H. B. Xiao, L. F. Xu, C. P. Yang, and Z. C. Xia, Sci. Rep. **6** (2016).
[16]   J. Nogues, D. Lederman, T. J. Moran, and I. K. Schuller, Phys. Rev. Lett. **76**, 4624 (1996).
[17]   R. Rana, P. Pandey, R. P. Singh, and D. S. Rana, Sci. Rep. **4** (2014).
[18]   A. P. Chen *et al.*, Adv. Mater. **29** (2017).
[19]   R. L. Stamps, J. Phys. D. **33**, R247 (2000).
[20]   S. Dong, K. Yamauchi, S. Yunoki, R. Yu, S. Liang, A. Moreo, J.-M. Liu, S. Picozzi, and E. Dagotto, Phys. Rev. Lett. **103** (2009).
[21]   F. Li, C. Song, Y. Y. Wang, B. Cui, H. J. Mao, J. J. Peng, S. N. Li, G. Y. Wang, and F. Pan, Sci. Rep. **5** (2015).
[22]   N. C. Koon, Phys. Rev. Lett. **78**, 4865 (1997).
[23]   Y. Ijiri, T. C. Schulthess, J. A. Borchers, P. J. van der Zaag, and R. W. Erwin, Phys. Rev. Lett. **99** (2007).
[24]   E. Folven, A. Scholl, A. Young, S. T. Retterer, J. E. Boschker, T. Tybell, Y. Takamura, and J. K. Grepstad, Nano Lett. **12**, 2386 (2012).
[25]   Y. Takamura, E. Folven, J. B. R. Shu, K. R. Lukes, B. Z. Li, A. Scholl, A. T. Young, S. T. Retterer, T. Tybell, and J. K. Grepstad, Phys. Rev. Lett. **111**, 107201 (2013).
[26]   D. Treves, J. Appl. Phys. **36**, 1033 (1965).
[27]   A. Monsen, J. E. Boschker, F. Macia, J. W. Wells, P. Nordblad, A. D. Kent, R. Mathieu, T. Tybell, and E. Wahlstrom, J. Magn. Magn. Mater. **369**, 197 (2014).
[28]   M. Huijben, L. W. Martin, Y.-H. Chu, M. B. Holcomb, P. Yu, G. Rijnders, D. H. A. Blank, and R. Ramesh, Phys. Rev. B. **78** (2008).
[29]   A. Scholl *et al.*, Science **287**, 1014 (2000).
[30]   F. Y. Bruno *et al.*, Nat. Commun. **6** (2015).
[31]   J. F. Ding, O. I. Lebedev, S. Turner, Y. F. Tian, W. J. Hu, J. W. Seo, C. Panagopoulos, W. Prellier, G. Van Tendeloo, and T. Wu, Phys. Rev. B. **87** (2013).
[32]   M. Vafaee, S. Finizio, H. Deniz, D. Hesse, H. Zabel, G. Jakob, and M. Klaui, Appl. Phys. Lett. **108** (2016).
[33]   H. Ohldag, A. Scholl, F. Nolting, E. Arenholz, S. Maat, A. T. Young, M. Carey, and J. Stohr, Phys. Rev. Lett. **91**, 017203 (2003).
[34]   W. H. Meiklejohn, J. Appl. Phys. **33**, 1328 (1962).
[35]   J. W. Seo, E. E. Fullerton, F. Nolting, A. Scholl, J. Fompeyrine, and J. P. Locquet, J. Phys.-Condens. Mat. **20** (2008).
[36]   C. Sterwerf, Ph.D. thesis, Bielefeld University, 2016.
[37]   E. Arenholz, G. van der Laan, F. Yang, N. Kemik, M. D. Biegalski, H. M. Christen, and Y. Takamura, Appl. Phys. Lett. **94** (2009).
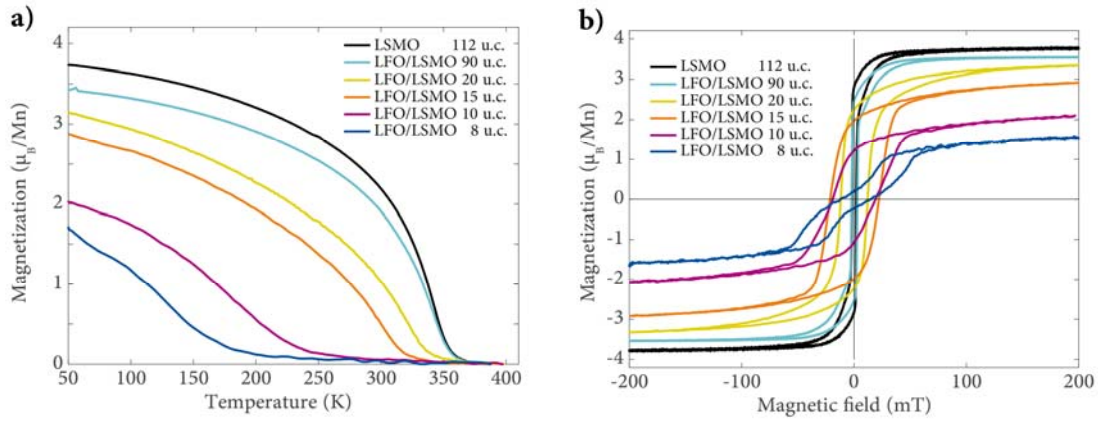
Figure 1: a) Saturation magnetization as function of temperature, measured during gradual heating in a field of 200 mT, after field cooling in 3 T from 400 K and b) hysteresis loops of as-grown samples measured at 50 K after cooling in zero field. The moment is normalized to Bohr magnetons (μ_B) per Mn ions in the LSMO layer.
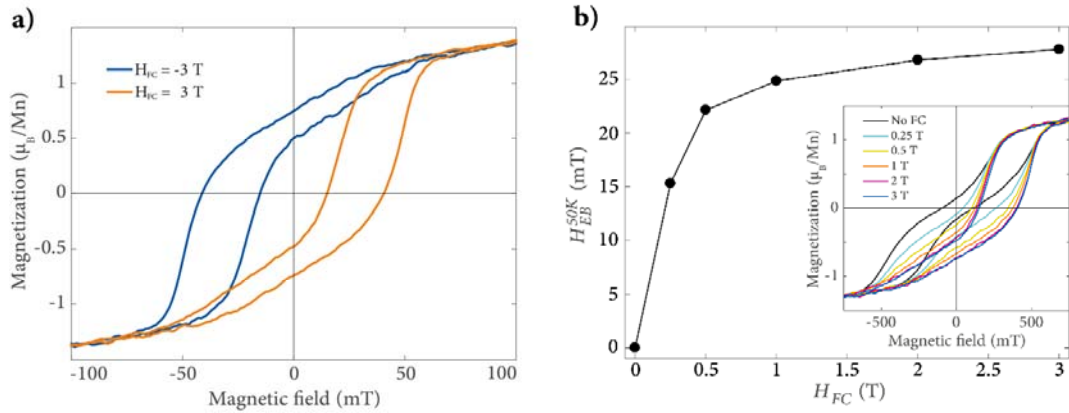

Figure 2: Exchange bias measured after field cooling, shown for the LFO (10 u.c.)/LSMO (8 u.c.) sample. a) shows hysteresis loops measured at 50 K after field cooling in 3 T fields from 400 K and b) exchange bias obtained at 50 K as function of cooling field strength, where field cooling is performed from 400 K. The solid line is meant as a guide to the eye. The inset in b) shows the hysteresis loops measured at 50 K.
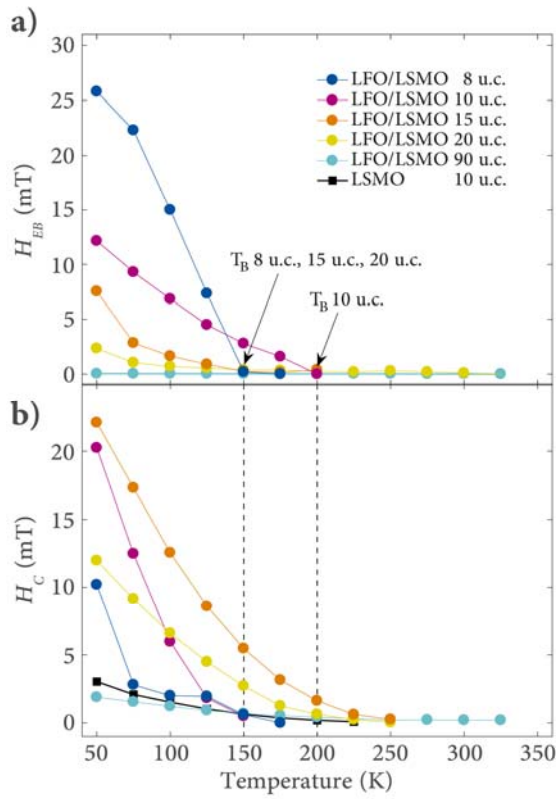
Figure 3: Temperature dependence of a) exchange bias and b) coercivity in the LFO/LSMO heterostructures as function of increasing temperature, measured after field cooling in 3 T from 400 K. The solid lines are meant as a guide to the eye. Approximate values of T_B for the heterostructures are indicated in (a) and the coercive field for the 10 u.c. LSMO single layer sample is included for reference in (b). The dashed lines are meant as a guide to the eye.
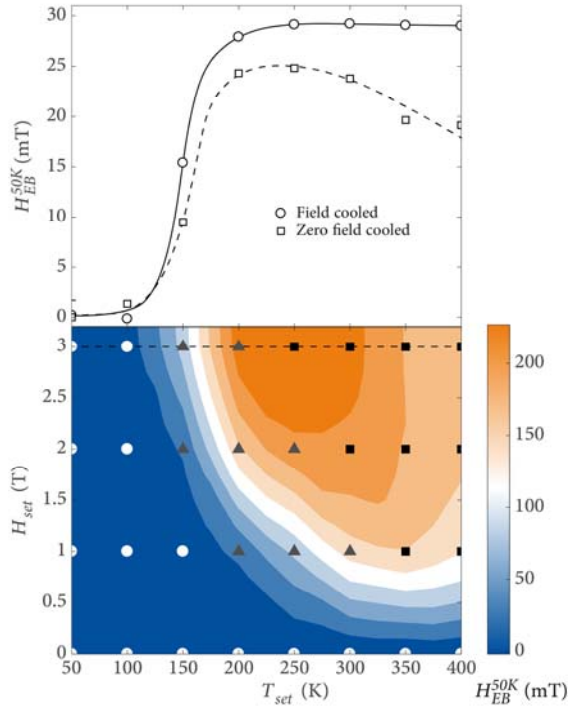
Figure 4: H_{EB}^{50K} measured after applying a setting field H_{set} at a temperature T_{set} and zero field cooling to 50 K (lower panel). The color grading is based on interpolation between the data points and serves as a guide to the eye. Symbols indicate the three regimes; frozen (white circles), intermediate (grey triangles) and saturation (black squares). The EB is reset by field cycling at 400 K in between each measurement. The data points indicated by the dashed line in the lower panel is shown in the upper panel (squares) together with exchange bias measured at 50 K after field cooling in 3 T (circles) from T_{set}. The solid and dashed lines in the upper panel are guides to the eye.
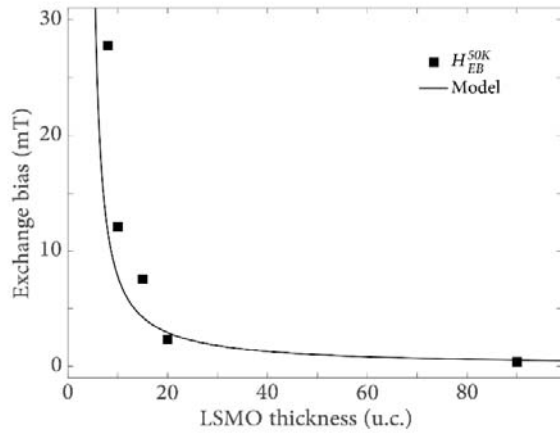
Figure 5: Exchange bias as function of LSMO layer thickness, with data points measured at 50 K after field cooling in 3 T from 400 K. The solid line represents the Meiklejohn & Bean model, calculated with the average σ_{int} of 10.6 µJ/m². A magnetic dead layer of 4 u.c. in LSMO has been accounted for in the calculations.
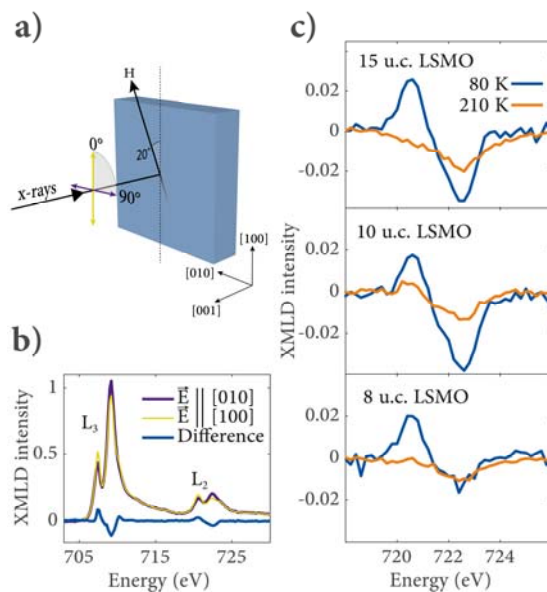

Figure 6: a) Schematic of the XMLD measurement geometry. b) XAS spectra for the LFO (10 u.c.) / LSMO (15 u.c.) heterostructure obtained at 80 K for two linear polarizations, together with XMLD difference. c) Difference in dichroism signal at the L_2 edge for heterostructures with different LSMO layer thickness, obtained at 80 K and 210 K.
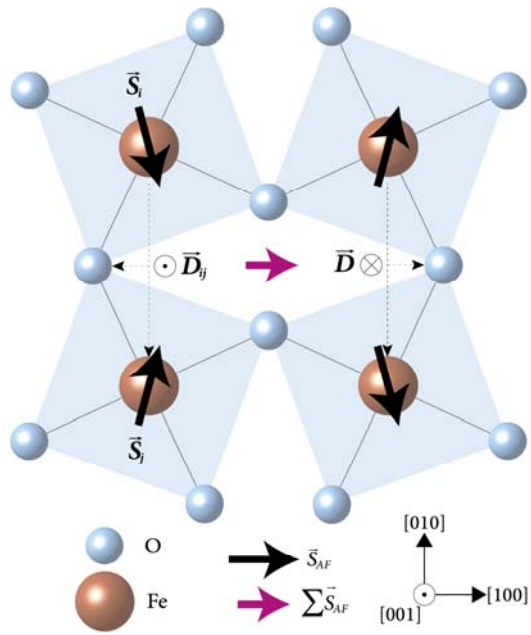
Figure 7: Illustration of octahedral rotations around the [001] axis, causing spin canting in the (001) plane in LFO due to Dzyaloshinkii-Moriya interactions. The staggered $\vec{D}$-vectors together with the G-type AF order cause a net spin moment in the [100] direction, indicated by the purple vector.